

Measurements of Electron-Pair-Production Cross Sections*

Munaim Mashkour

Illinois Institute of Technology, Chicago, Illinois 60616

(Received 10 January 1973)

A number of cross sections associated with electron pair production have been measured in the photon energy range 10–300 MeV in Ilford G-5 emulsion ($Z_{\text{eff}} \approx 21$). Measurements include the distribution of the recoil momentum and scattering angle of the target nucleus, the divergence angle between the pair members, the energy partition, the effect of photon polarization, and the absolute pair production cross section. Agreements and disagreements with the theory and previous measurements are discussed.

I. INTRODUCTION

There is continuing interest in improving the understanding of pair production by moderate energy photons in the partially screened Coulomb fields of intermediate- and high- Z nuclei. Recent theoretical work, based on extensive computer calculations, has shown that the older estimates, which relied on Born, point-Coulomb, and Bethe-Maximon approximations could lead to serious errors.¹ The present work is an experimental contribution to this problem. We report detailed results on pair production in Ilford G-5 emulsion whose effective Z for this process is very nearly 21 (see Barkas¹⁷). The incident photon energies range from 10 to 300 MeV. These photons were derived from the magnetic bremsstrahlung (synchrotron radiation) which is generated when high-energy electrons (19 GeV) traverse pulsed MG fields (1.5 MG). All characteristics of this radiation can be accurately determined and this facilitates the interpretation of the experimental results.

We begin by briefly reviewing some of the most recent experiments on pair production. Due to the scope of the present work, we mention only those experiments where the conversion process takes place in the vicinity of an atomic nucleus. Sandhu *et al.*² reported results on the energy partition and divergence-angle distribution between the two members of an electron pair, in the photon energy range 5–90 MeV. Emigh³ reported on the distribution of the energy partition in the photon energy range 50–300 MeV. Hart *et al.*⁴ studied the distribution of the divergence angle in the photon energy range 50–200 MeV. Modesitt and Koch⁵ studied the distributions of the recoil momentum and scattering angle of the nucleus, in whose Coulomb field the pair creation takes place, for the photon energy range 1–19 MeV. Many of the previous measurements on the total pair production cross section were made near the threshold energy region. In particular, Yamazaki and Hollander⁶

made measurements on the total pair production cross section in the photon energy range 1.173–2.753 MeV, and observed that the Bethe-Heitler prediction gave too low a cross section in the lower part of the spectrum. Colgate⁷ reported good agreement with the Bethe-Heitler prediction at photon energies of 4.47 and 6.13 MeV. Chisholm and Nicholson⁷ reported good agreement with the calculations of Davies *et al.*⁷ of the pair production cross section when applied to Pb in the photon energy range 35–120 MeV. Earlier, Walker,⁸ Adams,⁹ and Lawson,¹⁰ measured the pair production cross section at photon energies of 11.04, 13.73, 17.6, 19.10, and 88 MeV, and observed that for heavy elements the Bethe-Heitler formulas predicted too high (up to 13%) a cross section. For completeness' sake, we note that high-energy pair production in hydrogen and deuterium has recently been measured by Rawlinson *et al.*¹⁰ and computed by Knasel.¹⁰

II. RADIATION SOURCE AND THE REGISTRATION OF PAIR PRODUCTION EVENTS

The present study is based on information derived from an experiment on the characteristic features of the synchrotron radiation (SR) produced by 19-GeV electrons deflected in 1.2- and 1.6-MG magnetic fields. A detailed report of this work, including particulars of the MG generators and the electron beam, will appear elsewhere.¹¹ Figure 1 shows a sketch of the principal components of the beam layout. Beam 1 corresponds to a test pulse that was registered before triggering the MG targets. Beam 2 was synchronized with the target field to yield the SR. The electron pair events were registered in Ilford G-5 nuclear emulsion plates, 600 μ thick. The particular emulsion plates that were analyzed (C plates in the figure) were oriented vertically with respect to the bremsstrahlung beam. Thus the materialized electron pairs propagate in a direction that is

essentially normal to the emulsion surface.

In the present work, many of the results are insensitive to the detailed theory of the SR. However, the photon polarization and the total radiation rate do affect the interpretation of the pair production polarization and the total pair production cross section. All our results are consistent with the assumption that the conventional classical relativistic theory of the SR is correct. Previous experiments on the SR, with electrons of 6.3 GeV energy and a field of 10 kG,¹² also showed good agreement with the theoretical predictions.

III. MEASUREMENT OF PAIR ENERGIES

The multiple scattering technique was utilized for the determination of the electron and positron energies.¹³ The vertical exposure facilitated a high scanning efficiency and increased scanning and measurement rates. This procedure, however, demands care in making appropriate corrections for emulsion distortion and in extracting the maximum information from the limited track length available. The emulsion distortion was evaluated, and subsequently subtracted from the raw data on the electron trajectories, by measuring the trajectories of some high-energy background electrons that were found to enter normal to the emulsion surface. To circumvent the limitations associated with the track lengths, information was derived from both scattering components of every track, rather than only one component as is usual in the analysis of horizontal tracks. Only those events which originated 10 μ from the top and 230 μ from the bottom of the unprocessed emulsions were chosen for detailed analysis.

Measurements were taken continuously along the track trajectories at average intervals of 10 μ . Subsequently, linear interpolation and extrapolation were used to define the scattering at constant cell lengths. A digitized Koritska microscope was used for the multiple scattering analysis. Measurements were made under 100 \times objective and 25 \times eyepiece. Scattering coordinates were determined through a remotely controlled micrometer. Pechan prisms were used for image rotation. This facilitated the interchange of the two scattering

components in the measurements. Data were recorded on magnetic tapes using a Datex tape recording system. A CDC 6600 computer was used for the data analysis.

A detailed description of the measurement procedure and the subsequent data analysis is given in a thesis.¹⁴

IV. DATA ANALYSIS

The limited track length available required the use of both scattering coordinates of each track. It was also necessary to develop the following computational procedure to make optimum use of the available information. For each track a primary cell length t_0 , corresponding to the average distance between the measured coordinate points, was defined. The cell length t was then allowed to range over all possible integral multiples of t_0 . At the same time a complete overlapping of cells was made.¹⁵ For each value of the cell length, the spurious scattering was deleted using the conventions of Voyvodic and Pickup.¹⁶ The difference-product technique¹⁷ was then employed to evaluate the noise-free multiple scattering signal, the measurement noise, and the standard deviation. The track rigidity could then finally be determined according to standard methods.¹⁷

This procedure yielded a range of rigidities corresponding to the different values of the cell lengths. The best values were selected according to a criterion discussed elsewhere.¹⁴ The uncertainties associated with the values of the rigidities that were finally chosen has averaged about 25%.

The method of "optimal track lengths"¹⁷ was employed for the determination of track directions. Specifically, the segments were defined with respect to the apparent origin of the pair creation, and the data within each segment were fitted to linear functions to yield the direction components. At a rigidity of 10 MeV/c the uncertainty in track directions averaged ± 0.023 rad; at 100 MeV/c the average uncertainty is ± 0.002 rad.

V. RESULTS

(i) The recoil momentum of each individual nucleus, in whose Coulomb field a pair creation took place, was determined from the constraints of energy and momentum conservation.⁵ The initial photon direction was determined to a precision of $\pm 5 \times 10^{-4}$ rad from the symmetry requirements on the distribution of the electron track directions with respect to the incident photon beam. In Fig. 2 we show histograms of the measured distributions for the photon energy range 10–300 MeV. Superimposed on these are the predictions of Jost *et al.*¹⁸ The theoretical curves and histograms are

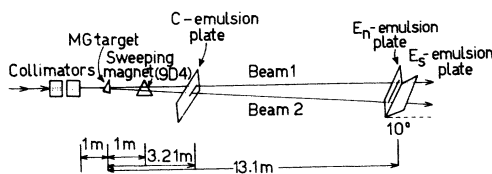


FIG. 1. Sketch of the electron-beam layout, MG target, emulsion plates, and the SR pattern.

normalized to equal areas. The Jost expression has been revised in accordance with the corrections noted by Borsellino.¹⁹ The atomic form factor entering this expression has been adapted from Bethe.²⁰

(ii) In Fig. 3 we show the distribution of the nuclear recoil angles. Superimposed on these are the theoretical predictions of Jost *et al.* The theoretical curves and histograms are also normalized to equal areas. We note that a 90° angle in this figure corresponds to a right-angle recoil with respect to the initial photon direction.

(iii) Figure 4 shows the distribution of the divergence angles between the two members of a pair. The abscissa in each diagram corresponds to the ratio ω/ω_0 , where ω is the divergence angle in radians and $\omega_0 = mc^2k/E_+E_-$. The dotted curves are derived from Borsellino's calculations.¹⁹ A correction noted by Hart *et al.*⁴ has been taken into account. The solid curves are of the form $C(\omega/\omega_0)/[1 + (\omega/\omega_0)^2]^2$ which is an adequate approximation for Bethe's expression.²⁰ The theoretical curves and histograms are again normalized to have equal areas.

(iv) Figure 5 shows the distribution of the energy partition between the two members of an electron-positron pair for the photon energy range 70–300 MeV. The theoretical curve corresponds to the Bethe-Heitler theory.²¹ The atomic screening functions $\phi_1(\gamma)$ and $\phi_2(\gamma)$, which enter the calculations, were evaluated according to Butcher

and Messel.²² In this figure, the theoretical curve has been normalized so that the central height is equal to the average heights of the central ten bins of the histogram.

VI. EFFECT OF PHOTON POLARIZATION ON PAIR PRODUCTION

The SR used for these studies has a marked elliptical polarization.²³ The relevant polarization parameter is a quantity $\pi(k)$, which is the ratio, at photon energy k , of the difference and the sum of the intensities of the two components of the radiation. In the present experimental arrangement, $\pi(k)$ when averaged over the photon energies in the range 15–100 MeV, turns out to be $\bar{\pi} = 0.76$.

The polarization of the radiation affects the geometrical distribution of the electron pairs. The simplest estimates of this effect can be derived from Wick's formula, which is based on the method of virtual quanta.²⁴ For high-energy photons, the differential cross section with respect to the azimuthal angle ϕ , made by the plane of the divergence angle of the electron pairs with respect to the polarization vector of the photon, is given by

$$\frac{d\sigma(\phi)}{d\phi} = C(1 + a \cos^2\phi), \quad (1)$$

where C is independent of ϕ , and $a = \frac{1}{3}$. We attempt to correlate the experimentally inferred

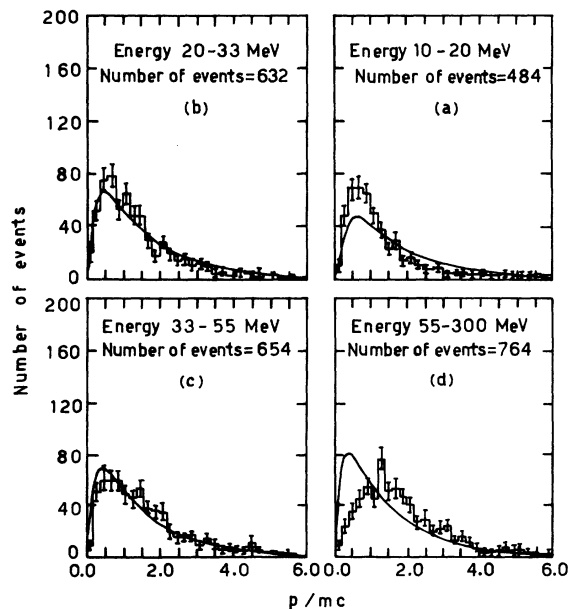


FIG. 2. Distribution of the recoil momentum of the nuclei. Theoretical curves are evaluated at photon energies 15, 27, 45, and 100 MeV, for *a*, *b*, *c*, and *d*, respectively. Theory due to Jost *et al.* (Ref. 18).

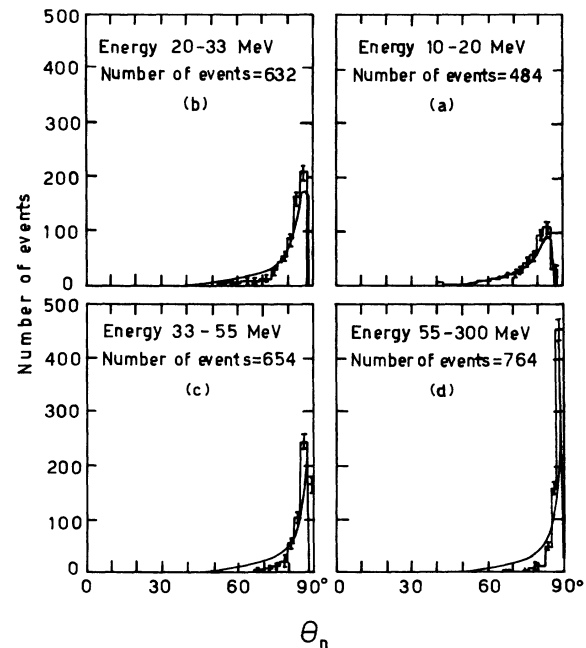


FIG. 3. Distribution of the recoil angles of the nuclei. Theoretical curves are evaluated at the same energies as in Fig. 2. Theory due to Jost *et al.* (Ref. 18).

values of a with the theoretical estimate of $\frac{1}{3}$. In the analysis, we will assume, however, that Eq. (1) represents the correct functional form.

The experimental distribution of the azimuthal angle ϕ due to both components of the SR can then be expressed as

$$\frac{dP(\phi)}{d\phi} = \frac{1}{2\pi} \left(1 + \frac{a\pi}{2+a} (1 - 2\sigma^2) \cos 2\phi \right), \quad (2)$$

where σ ($=0.35$ rad) is the over-all resolution of the measurements of the angle ϕ .¹⁴ The angle ϕ is measured relative to the dominant component of the radiation. Figure 6 shows the distribution of ϕ in the photon energy range 15–100 MeV, and a superimposed functional fit of the form $A + B \cos 2\phi$. A 10% contribution was subtracted from A , to correct for an isotropic background. Inserting the other known quantities, we find $a = 0.34 \pm 0.1$, as compared with $\frac{1}{3}$ from Wick's estimate.

VII. TOTAL PAIR PRODUCTION CROSS SECTION

A. Method of Analysis

By comparing the experimentally inferred intensity of the SR with the calculated values,^{23, 25} we could check the total pair production cross section in emulsion (Ilford G-5) in the photon energy range

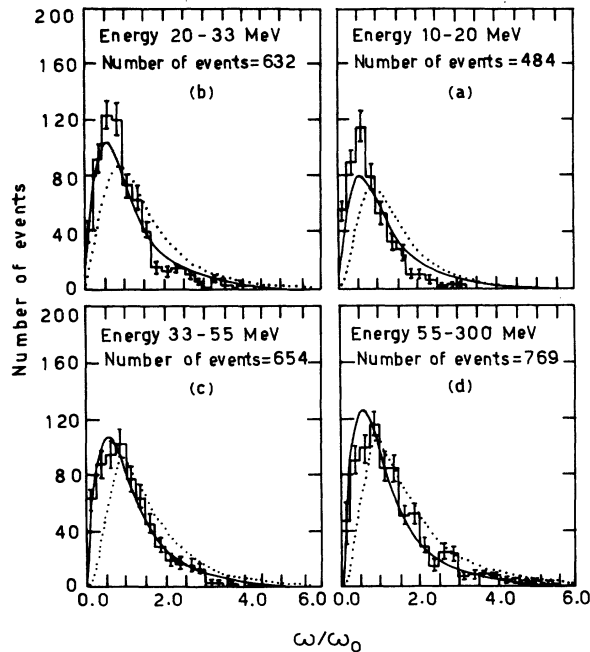


FIG. 4. Distribution of the divergence angle of the electron-positron pairs. Theoretical curves are evaluated at the same energies as in Fig. 2. Dotted curves derived from Borsellino (Ref. 19); solid curves correspond to Bethe approximation (Ref. 2.)

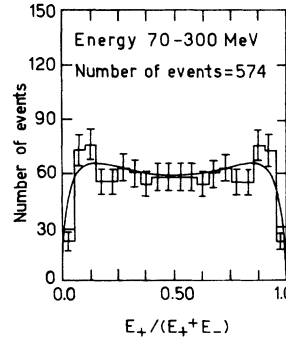


FIG. 5. Distribution of the energy partition between the two members of a pair. Theoretical curve is evaluated at a photon energy of 120 MeV. Theory due to Bethe and Heitler (Ref. 21).

10–100 MeV. A concise way of arriving at this result is to consider the ratios of the following experimental and theoretical quantities:

$$\frac{\sigma_{\text{expt}}(k)}{\sigma_{\text{theor}}(k)} = \frac{I_{\text{expt}}(k)}{I_{\text{theor}}(k)}, \quad (3)$$

where $\sigma_{\text{expt}}(k)$, $I_{\text{expt}}(k)$ and $\sigma_{\text{theor}}(k)$, $I_{\text{theor}}(k)$ denote the experimental and theoretical pair production cross sections and the corresponding spectral intensities at photon energy k . This analysis required the determination of a number of auxiliary quantities: The absolute electron-beam flux was obtained from direct counting of the electrons, which were incident on the emulsion plate. The absolute radiation intensity could then be determined from the geometry of the MG targets and the measured field strengths. The experimental radiation intensities are obtained from the measured electron pair spectrum by unfolding the "theoretical" total pair production cross sections. These theoretical pair production cross sections were computed from the numerical compilation of Storm and Israel,²⁶ by introducing appropriate weight factors corresponding to the composition of the emulsion.¹⁷

B. Correction for Scanning and Measuring Efficiency

It was established by a rescanning check and the study of failed events that most of the missed events corresponded to pairs with extremely asym-

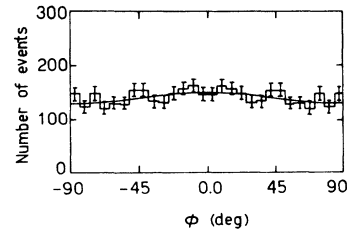


FIG. 6. Distribution of the azimuthal angle of the plane of divergence angle of the pairs about the initial photon direction. Curve is a functional fit of the form $A + B \times \cos 2\phi$.

metric energy partition. Therefore, we could estimate the number of missed events through the use of the theoretical energy partition distribution, from the number of events whose members had comparable energies. This procedure of course relies on the assumption that the Bethe-Heitler calculation²¹ of the energy partition distribution is correct in the appropriate energy range (10–100 MeV). A detailed discussion of this procedure is given in Ref. 14. Table I gives a summary of the correction factors.

C. Subtraction of Background Radiation: Results

The particular beam configuration employed permitted a sizable Coulomb bremsstrahlung background to contaminate the SR signal. At 10 MeV, background/signal was about 4%; at 100 MeV this ratio increased to about 25%. However, the background contribution could be reliably identified and subtracted from the SR signal, by exploiting the fact that the Coulomb bremsstrahlung was not as sharply localized on the emulsions as the SR.

Once these correction factors were taken into account, we could determine the right-hand side of Eq. (3) at the different energy intervals, in the range 10–100 MeV. Figure 7 shows the results averaged over the two exposures that were analyzed. The wedge lines reflect an uncertainty in addition to the statistical limitations, which is associated with the absolute field calibration ($\pm 5\%$). Below 50 MeV the results are insensitive to this source of error.

VIII. CONCLUSIONS

The results presented in Figs. 2–4 are largely insensitive to scanning efficiency corrections. Furthermore, the inclusion of variations in the measurement resolution of various parameters makes an insignificant change in the theoretical spectra. The emulsion analysis therefore leads to the following statements in relation to these properties. In Fig. 2, the small momentum transfer

TABLE I. Scanning and measuring efficiency.

| Photon energy interval (MeV) | Correction factor ^a | Direct efficiency check (%) | Photon energy interval (MeV) | Correction factor | Direct efficiency check (%) |
|------------------------------|--------------------------------|-----------------------------|------------------------------|-------------------|-----------------------------|
| 10–15 | 1.29 | 71 | 30–40 | 1.15 | 93 |
| 15–20 | 1.57 | 71 | 40–50 | 1.21 | 94 |
| 20–25 | 1.26 | 86 | 50–70 | 1.01 | 90 |
| 25–30 | 1.18 | 92 | 70–100 | 1.04 | 97 |

^a Obtained from a study of the energy partition.

^b Derived from rescanning checks (300 events) and the study of failed events.

tails of the spectra are heavily influenced by the screening effects of the electron shells. We note a marked disagreement between theory and experiment at high photon energy. However, at lower energies we observe a good correlation with the theory, contrary to the results reported by Modesitt and Koch.⁵ A similar correspondence with the theoretical predictions is observed for the recoil angle of the nuclei: The results for the distribution of the divergence angle follow approximately those of Sandhu² and Hart.⁴ However, we do not find clear evidence for a systematic shift of the peak of the distributions towards larger angles, as reported by Sandhu.⁵ We note that the agreement with Borsellino's expression over the entire range 10–300 MeV is poor.

On the other hand, there is a good agreement between the theoretical and experimental energy partition distribution in the photon energy range 70–300 MeV. In this region, the measurement and scanning efficiency checks show 97% efficiency. This value is well in accord with the correspondence between theory and experiment. The screening effect of the electron shells is clearly manifested by the central dip of the distribution.

The Wick formula gives an adequate description of the effect of the photon polarization on the pair production. Under the present experimental conditions, the polarization gives rise to a rather small effect. Figure 6 indicates that the pair members are preferentially correlated with the plane defined by the polarization vector and the initial photon direction.

There is fair agreement between the present experimental total pair production cross section and the theoretical values inferred from the Storm-Israel tabulation. The deviations indicated on Fig. 7 can be attributed to a 5% statistical spread as

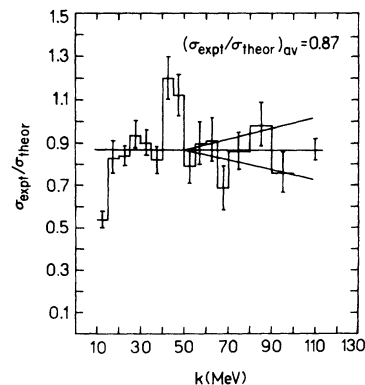


FIG. 7. The ratio $\sigma_{\text{expt}}(k)/\sigma_{\text{theor}}(k)$ as a function of the photon energy. Wedge lines indicate the (nonstatistical) uncertainty in the evaluation owing to an imprecision ($\pm 5\%$) of the magnetic field calibration.

well as uncertainties associated with the calibration of the MG-target field.

ACKNOWLEDGMENTS

It is a pleasure to thank Professor T. Erber for his kind encouragement and numerous helpful suggestions and remarks. My thanks and appreciation also go to Dr. H. Heckman, whose guest I was while carrying out the emulsion analysis at the

Lawrence Berkeley Laboratory. I am grateful for his kind hospitality, his generous supply of equipment, and his many helpful suggestions. Professor F. Herlach and R. McBroom were responsible for the design and operation of the MG targets. Dr. D. Greiner introduced me to the multiple scattering technique. The efforts of the Stanford Linear Accelerator staff, particularly Dr. J. J. Murray and Dr. R. Gearhart, are also gratefully acknowledged.

*Supported by the National Science Foundation.

¹J. Motz, H. Olson, and H. Koch, *Rev. Mod. Phys.* 41, 581 (1969); J. K. Fink and R. H. Pratt, *Phys. Rev.* (to be published).

²H. Sandhu, E. Webb, R. Mohanty, and R. Roy, *Phys. Rev.* 125, 1017 (1962).

³C. Emigh, *Phys. Rev.* 86, 1028 (1952).

⁴E. Hart, G. Cocconi, and M. Sellen, *Phys. Rev.* 115, 678 (1959).

⁵G. Modesitt and H. Koch, *Phys. Rev.* 77, 175 (1950).

⁶T. Yamazaki and J. Hollander, *Phys. Rev.* 140, 630 (1965).

⁷S. Colgate, *Phys. Rev.* 87, 592 (1952); A. Chisholm and J. P. Nicholson, *J. Phys. A* 5, 1404 (1972); H. Davies, H. Bethe, and L. Maximon, *Phys. Rev.* 93, 768 (1954).

⁸R. Walker, *Phys. Rev.* 76, 527 (1948).

⁹G. Adams, *Phys. Rev.* 74, 1707 (1948).

¹⁰J. Lawson, *Phys. Rev.* 75, 433 (1949); W. R. Rawlinson *et al.*, *Nucl. Phys. B* 45, 41 (1972); T. M. Knasel, DESY Reports No. 70/2 and 70/3 (Hamburg, 1970) (unpublished).

¹¹T. Erber *et al.* (unpublished).

¹²G. Bathow, E. Freytag, and R. Haensel, *J. Appl. Phys.*

37, 3449 (1966).

¹³P. Fowler, *Philos. Mag.* 41, 86 (1950).

¹⁴M. Mashkour, Ph.D. thesis (Illinois Institute of Technology, 1972) (unpublished).

¹⁵D. Greiner, physics notes (Lawrence Berkeley Laboratory, 1969) (unpublished).

¹⁶L. Voyvodic and P. Pickup, *Phys. Rev.* 85, 91 (1952).

¹⁷W. Barkas, *Nuclear Research Emulsion* (Academic, New York, 1963), Vol. I.

¹⁸R. Jost, J. Lutinger, and M. Slotnick, *Phys. Rev.* 80, 189 (1950).

¹⁹A. Borsellino, *Phys. Rev.* 89, 1023 (1953).

²⁰H. Bethe, *Ann. Phys. (Leipz.)* 5, 325 (1930).

²¹H. Bethe and W. Heitler, *Proc. R. Soc. (Lond.) A* 166, 83 (1934); H. Davies, H. Bethe, and L. Maximon, *Phys. Rev.* 87, 156 (1952).

²²J. Butcher and H. Messel, *Nucl. Phys.* 20, 15 (1960).

²³A. Sokolov and I. Ternov, *Synchrotron Radiation* (Akademie-Verlag, Berlin, 1968).

²⁴G. Wick, *Phys. Rev.* 81, 467 (1951).

²⁵T. Erber, *Rev. Mod. Phys.* 38, 626 (1966).

²⁶E. Storm and H. Israel, *Nucl. Data Tables* 7, 565 (1970).